

Review

The Revolutionary Roads to Study Cell–Cell Interactions in 3D In Vitro Pancreatic Cancer Models

Donatella Delle Cave ¹, Riccardo Rizzo ², Bruno Sainz, Jr. ^{3,4}, Giuseppe Gigli ^{2,5}, Loretta L. del Mercato ² and Enza Lonardo ^{1,*}

¹ Institute of Genetics and Biophysics “A. Buzzati-Traverso”, National Research Council (CNR-IGB), Via Pietro Castellino 111, 80131 Naples, Italy; donatella.dellecave@igb.cnr.it

² Institute of Nanotechnology, National Research Council (CNR-NANOTEC), c/o Campus Ecotekne, via Monteroni, 73100 Lecce, Italy; riccardo.rizzo@nanotec.cnr.it (R.R.); giuseppe.gigli@unisalento.it (G.G.); loretta.delmercato@nanotec.cnr.it (L.L.d.M.)

³ Department of Cancer Biology, Instituto de Investigaciones Biomedicas “Alberto Sols” (IIBM), CSIC-UAM, 28029 Madrid, Spain; bsainz@iib.uam.es

⁴ Spain and Chronic Diseases and Cancer, Area 3-Instituto Ramon y Cajal de Investigacion Sanitaria (IRYCIS), 28029 Madrid, Spain

⁵ Department of Mathematics and Physics “Ennio De Giorgi”, University of Salento, via Arnesano, 73100 Lecce, Italy

* Correspondence: enza.lonardo@igb.cnr.it

Simple Summary: Pancreatic cancer is an extremely lethal malignancy with a survival rate lower than any other cancer type. For decades, two-dimensional (2D) cultures have been the cornerstone for studying cancer cell biology and drug testing, due to their simplicity and cost. However, their inability to reconstitute the tumor architecture, the absence of nutrient and oxygen supply gradients, as well as the lack of appropriate mechano-forces that mimic the extracellular microenvironment, make them an inadequate model to accurately reproduce tissue level-specific characteristics. Bioengineering systems, such as three-dimensional (3D) patient-specific models, are progressively emerging as systems better able to mimic the biology of pancreatic tumors and to test new anticancer therapies, as they more efficiently recapitulate the complex tumor microenvironment characteristic of pancreatic tumors. Here, we review how cellular component interactions, within the pancreatic tumor microenvironment, have been studied and mimicked in 3D cell culture models, and discuss selected emerging therapeutic strategies, addressing their limitations and future perspectives.

Abstract: Pancreatic cancer, the fourth most common cancer worldwide, shows a highly unsuccessful therapeutic response. In the last 10 years, neither important advancements nor new therapeutic strategies have significantly impacted patient survival, highlighting the need to pursue new avenues for drug development discovery and design. Advanced cellular models, resembling as much as possible the original in vivo tumor environment, may be more successful in predicting the efficacy of future anti-cancer candidates in clinical trials. In this review, we discuss novel bioengineered platforms for anticancer drug discovery in pancreatic cancer, from traditional two-dimensional models to innovative three-dimensional ones.

Keywords: pancreatic cancer; 3D cultures; tumor microenvironment; fluorescent microscopy; nanotechnology; predictive models



Citation: Delle Cave, D.; Rizzo, R.; Sainz, B., Jr.; Gigli, G.; del Mercato, L.L.; Lonardo, E.

The Revolutionary Roads to Study Cell–Cell Interactions in 3D In Vitro Pancreatic Cancer Models. *Cancers* **2021**, *13*, 930. <https://doi.org/10.3390/cancers13040930>

Academic Editor: Marilena Loizidou

Received: 19 January 2021

Accepted: 18 February 2021

Published: 23 February 2021

Publisher’s Note: MDPI stays neutral with regard to jurisdictional claims in published maps and institutional affiliations.



Copyright: © 2021 by the authors. Licensee MDPI, Basel, Switzerland. This article is an open access article distributed under the terms and conditions of the Creative Commons Attribution (CC BY) license (<https://creativecommons.org/licenses/by/4.0/>).

1. Introduction

Pancreatic cancer (PC) is a devastating and essentially incurable disease, leading to patient death in the majority of cases [1]. Incidence and mortality are increasing steadily, and PC is predicted to become the second leading cause of cancer-related death by 2030 [2]. According to the Italian Association of Medical Oncology (AIOM), in 2019, approximately 13,500 new PC cases were diagnosed in Italy [3]. These dramatic numbers are due largely

to late diagnosis, lack of effective therapies, and a poor understanding of PC biology. Thus, PC has become a world healthcare priority, and studies focused on novel *in vitro* models to investigate tumor progression and develop more effective treatments are urgently needed. One reason for the lack of success for the majority of drugs used to treat PC patients is their inappropriate purposing and associated toxicity. At the preclinical stage, two-dimensional (2D) cultures have been a milestone in the study of cancer biology, since they represent a useful platform for analyzing genetic and molecular alterations and a cost-effective system for drug screening [4]. However, they are an inherently and extremely simplified model that fail to precisely reflect the human tumor microenvironment (TME) and its molecular components [5], which can inevitably lead to non-translatable results [6,7]. Those aspects are crucial for the study of PC, characterized by an abundant desmoplastic core, which accounts for up to 90% of the total tumor volume, and by an intricate cross-talk among tumor and stromal cell, both of which are critical aspects for cancer progression [8,9]. The TME is a very complex ecosystem in which several cellular (such as pancreatic stellate cells (PSCs), cancer-associated fibroblasts (CAFs), and immune cells) and non-cellular components (such as cytokines, immunoregulatory molecules, and extracellular matrix (ECM) components) are involved, contributing to the development of a hypoxic and “cold” immunosuppressive tumor, resistant to chemotherapy, targeted therapy, and immunotherapy [10]. While the number of drugs targeting the TME is progressively increasing, there is an urgent demand for more biologically and physiologically relevant *in vitro* preclinical models that can accurately mimic the TME that exists in patient tumors. The limitations of 2D models have been, in part, overcome by the use of genetically engineered mouse models (GEMMs), which recreate the most frequent genetic alterations associated with pancreatic cancer progression and provide a more physiological microenvironment for drug testing and genetic research [11]. However, *in vivo* studies are expensive, time-consuming, and ethically not suitable for drug screening and, most important, the results obtained have limited relevance in humans [12]. The opportunity of reproducing the TME *in vitro* by growing tumor cells in three-dimensional (3D) matrixes or scaffolds has opened new horizons in the field of drug testing. These 3D *in vitro* tumor models have been shown to be superior to 2D models, allowing for multiple cell populations to interact and mimicking the complexity and the biomechanical properties of tumors as well as tumor heterogeneity, and allowing for treatment responses similar to those seen in patients diagnosed with PC [13–17].

2. 3D In Vitro Models

3D *in vitro* systems are advantageous predictive tools, which may accelerate translating basic research into personalized medicine by providing more physiological information on cellular responses to different stimuli [18].

2.1. Spheroid

Spheroids are the simplest 3D model, which can be generated by the hanging drop technique, consisting of embedding cells in different matrices (such as collagen, methylcellulose, gelatin, and alginate hydrogels), or by growing single-cell suspensions in ultra-low attachment plates, in order to minimize the adhesion to plastic supports and to optimize cell–cell and cell–matrix interactions [19]. Spheroids can arise from self-assembling cells or via cellular aggregation and constitute an easy and highly reproducible 3D model [20]. Recently, Cavo and colleagues developed a new method to generate spheroids from the pancreatic ductal adenocarcinoma (PDAC) cell line (i.e., MiaPaCa2) with the hanging drop technique. They used a methylcellulose-enriched media and hydrophobic substrates to generate well-organized pancreatic spheroids with increased mesenchymal and cancer stem cell features [21]. This method appears to be efficient for the long-term generation of spheroids, even from those cell lines that hardly give rise to 3D structures due to low cohesiveness (Figure 1a). By comparing 2D cultures with 3D spheroids generated by different techniques (e.g., ultra-low adhesion concave microwells, Matrigel inclusion, and organ-

otypic systems), Zeeberg and colleagues found differences in cell growth, morphology, and in the response to different stimuli. They concluded that the organotypic culture, generated by plating cells on the top of a matrix gel, more closely recapitulated the tissue architecture of PC [22].

2.2. Patient-Derived Organoids (PDOs)

PDOs are 3D structures established from freshly isolated primary cells, which retain the ability of self-renewal and self-organization in an organ-like structure that recapitulates the tissue of origin. A pioneer study in establishing pancreatic organoids from both normal and freshly isolated human tumor biopsies was performed by Boj et al. [23]. The authors optimized the standard culture condition protocols for generating organoids able to recapitulate disease-specific alterations, enabling them to recreate in vitro the different stages of tumor progression. Specifically, single-cell suspensions are embedded in a Matrigel or collagen matrix and supplemented with a media containing a well-defined combination of tissue-specific growth factors [23–25]. PDOs can be genetically engineered in vitro by CRISPR-Cas9 (Clustered Regularly Interspaced Short Palindromic Repeats) technology to specifically edit tumor-driving genes, and can be xenografted in immunodeficient mice for in vivo studies [26].

The potential of pancreatic PDOs has also been recently exploited for the development of a PDO-based gene expression signature [27] and for the establishment of PDO biobanks [28]. PDOs represent a powerful model to recapitulate tumor histology and for personalized drug screening. Intriguingly, Seino and colleagues identified three functional PDO subtypes in PDAC on the basis of differences in stem cell niche factor dependency. By engineering them with clustered regularly interspaced short palindromic repeats (CRISPR)-Cas9 technology, they found that exogenous WNT is required to support the initial stages of tumorigenesis but it is dispensable in the late stage of tumor progression [29]. Pancreatic PDOs have also been shown to be as effective at determining drug efficacy compared to more labor-intensive and cost-prohibitive in vivo patient-derived xenograft (PDX) models. For example, Frappart et al. published a small-scale drug screening PDO platform that was successfully validated in an in vivo xenograft trial, highlighting the clinical utility of PDOs for validating and discovering new treatments for PC [30] (Figure 1b). Moreover, Nelson et al. used different multidisciplinary approaches, which included confocal microscopy and transcription profiling analysis, to compare PDX organoids with isogenetically matched 2D primary cell lines from PDAC tumors and primary cell line organoids (CLOs) [31]. Interestingly, they developed an in vitro method to generate CLOs, which very closely recapitulated the main features of organoids generated from PDXs, thus overcoming the limitations associated with xenografts. Along these lines, PDO drug screening platforms have recently been improved by the development of automated organoid-based platforms that take advantage of microfluidic systems for the simultaneous and time-controlled test of thousands of compounds, enabling real-time genetic and phenotypic analysis of PDOs, serving as a step forward in personalized therapy [32].

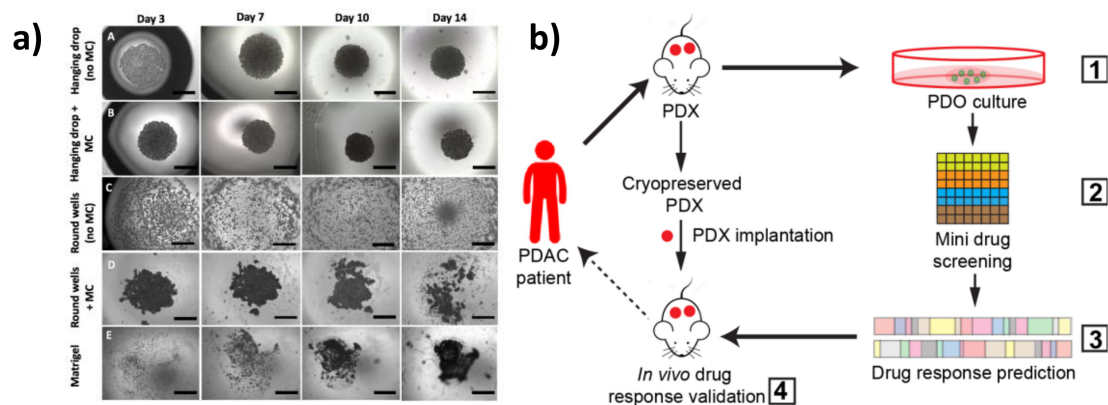


Figure 1. Three-dimensional (3D) in vitro models of pancreatic cancer. (a) MiaPaCa-2 spheroid growth using different methods. Scale bars = 1000 μm (adapted from [21]). (b) Schematic representation of the patient-derived organoid (PDO)-derived system. (1) Generation of PDO and patient-derived xenograft (PDX) models from cryopreserved xenografts of patients with pancreatic ductal adenocarcinoma (PDAC). Screening of Food and Drug Administration (FDA)-approved drugs (2) and validation in organoid cultures (3). Selection of effective drugs for small-scale drug screenings and validation in the PDXs (4) (adapted from [30]).

3. Reconstitution of Tumor Cell Heterogeneity and Complexity in 3D In Vitro Models

PC is characterized by a dense desmoplastic reaction defined by different cellular components, such as immune cells, fibroblasts, endothelial cells, and PSCs, dispersed in an organized extracellular matrix enriched in collagens, hyaluronic acid, and laminins [33,34]. The TME is therefore conditioned by distinct environmental factors, i.e., cytokines, growth factors, as well as a specific biochemical profile, which mediate cellular communication and are crucial in influencing cancer progression [35,36]. Reconstituting the tumor complexity by using 3D models requires taking into consideration the specific interactions between matrix components and the different cellular types present in the tumor in order to recreate in vitro the specific environmental conditions that distinguish each tumor. Attempts to recreate such a complex environment is also one of the ways to master in vitro tumor modeling.

3.1. Scaffolds

An optimal scaffold should offer a suitable environment for cell growth and allow for the development of in vitro tumor models that thoroughly recapitulate cell–extracellular matrix exchanges. In this scenario, tumor cells can be cultivated within biomaterials, including de-cellularized native tissues or in 3D synthetic and/or natural scaffolds. The biophysical properties of 3D structures are critical aspects for the study of PCs, as demonstrated by Puls et al., who generated a 3D PC model by embedding PDAC cells into different matrices obtained from type I collagen and Matrigel at various percentages. The authors found that matrix stiffness causes epithelial to mesenchymal transition (EMT) and induces the growth of cells as tight clusters [37]. Chiellini et al. developed a 3D model in which PDAC cells were embedded in a hydrogel made of chitosan (mCS) or a polyelectrolyte complex (mPEC) between CS and poly(g-glutamic acid) (g-PGA). These systems allowed for the generation of spheroids with enhanced features associated with cancer invasiveness [38]. Ricci et al. generated scaffolds by combining different polymeric formulations and different techniques in an attempt to reproduce various structures and ECM features, as well as to test their influence on tumor growth. They found that spongy scaffolds obtained via emulsion-based and salt leaching-based techniques increased cell viability and aggressiveness by inducing a spatial organization of tumor cells that closely recapitulated those found in vivo [39]. The advancements in the field of tissue engineering (TE) have facilitated the use of scaffold-based 3D culture systems in which cells are induced to colonize rigid micro- or macro-porous structures made of natural or synthetic fibers that mimic the ECM

architecture [40]. Scaffold can be synthesized by modulating different parameters, such as stiffness and porosity, in order to sustain cell viability and to mimic the morphology of the original tissue [41,42]. To better reproduce the TME architecture, Totti et al. developed a porous polyurethane scaffold coated with fibronectin, one of the main components of the extracellular matrix, and they showed that this system enhanced long-term tumor proliferation and collagen-I production compared to uncoated scaffolds, as well as induced a spatial oxygen and nutrient gradient [42].

3.2. 3D Cell/TME

Although 3D cultures have significantly improved the analysis of cancer progression and drug response, compared to 2D cultures, they are still far from recapitulating the complexity of the TME *in vitro*. The heterotypic 3D tumor culture, obtained by co-culturing different cell types, provides a suitable system that reflects the physiological properties of PDAC tumors and a more realistic response to chemotherapeutic treatment [43,44]. As mentioned above, PDAC is characterized by a dense and fibrotic stroma, mainly composed by PSCs, which are quiescent cells that upon activation secrete abundant ECM proteins such as fibronectin and collagen [45]. The involvement of the stroma in PDAC chemoresistance has been widely debated and researched [46]. It has been demonstrated to act as a supportive niche for PDAC cells, promoting their aggressiveness [47] and blocking chemotherapeutic drugs from reaching the tumor [34]. However, depletion of the stroma by the sonic hedgehog inhibitor (i.e., saridegib) in clinical trials has proven to produce more aggressive tumors and lower survival, which was also confirmed by three independent animal studies) [48,49]. A deeper understanding of the stroma and its crosstalk with the tumor cells is urgently needed. Towards this end, Norberg and colleagues developed a simple spheroid assay by co-culturing tumor and PSCs, both from human and mouse PDAC samples, in methylcellulose, followed by a “virtual sorting” to analyze the cross-talk between these two populations by using species-specific primers [50]. They found that the presence of stromal cells induced a mesenchymal phenotype and stimulated the proliferation of PDAC cells. In a different approach, Kim et al. co-cultured, in a microchannel device, PSCs and tumor spheroids generated from two different PDAC cell lines (with a mesenchymal and an epithelial phenotype, respectively) embedded in a collagen matrix. They observed differences in cell plasticity, extracellular matrix remodeling and migratory capacities on the basis of the PDAC cell types used for the co-culture [51] (Figure 2a). Broekgaarden et al. demonstrated that patient-derived CAFs increase PDAC resistance to oxaliplatin and benzoporphyrin derivative-mediated photodynamic treatment (PDT), both *in vitro* and *in vivo*, through the regulation of redox status [52]. This could be a useful tool for screening new drugs that modulate metabolic pathways. Karimnia et al. created a 3D model where PSCs were embedded in Matrigel that was overlaid with a single-cell suspension of PDAC cells, and they used this system to test oxaliplatin and PDT treatment [53]. They found that the PDAC cells were more resistant to chemotherapy and more sensitive to PDT treatments when co-cultured with fibroblast. This system allowed for a more physiological response assessment to drug treatments compared to homotypic cultures, suggesting that the PDT treatment could be used as a powerful approach for stroma depletion (Figure 2b) [53]. The lack of vasculature in the 3D models has been overcome by the generation of a multicellular 3D system, which combines tumor and stromal cells with microvascular endothelial cells exposed to shear stress and flow rates (Figure 2c–f). Transcriptome analyses revealed how this system closely mimics the true biology of the tumor [54]. In a 3D organotypic culture of endothelial, tumor, and stromal cells, Di Maggio et al. founded that PDAC, as well as a collagen-rich gel, suppressed the pro-angiogenic role of PSCs on endothelial cells, thus inhibiting their proliferation. This appears to be a valid model for testing the effect of anticancer drugs on tumor vascularity [55]. The tri-culture system was optimized by Gupta et al., who established a polyurethane (PU) scaffold-based model in which tumor cells were seeded in an inner compartment coated with fibronectin, surrounded by an external collagen-coated compartment containing stromal cells. This system allowed for

the activation of PSCs and the trans-migration between the two compartments [56]. Fook Lun Lai et al. generated a 3D vascularized network by engineering a co-culture, consisting of human PDOs, fibroblasts, and endothelial cells, on a perfusable platform that allows for the study of cell metabolic activity and drug screening [57]. PDAC consists of an extremely immunosuppressive microenvironment, and in order to study its contribution to chemotherapy resistance, Tsai and colleagues developed a multi-cellular organotypic model with stroma, tumor, and immune cells, which mimicked authentic TME interactions and was shown to be suitable for translational medicine in vitro [58]. Kuen et al. demonstrated the in vitro differentiation of monocytes into M2-like macrophages when grown in a 3D spheroid model, which included PDAC cells and fibroblasts [59]. This model could be used to analyze the tumor–stroma crosstalk influenced by the immune system. Finally, Ohlund and colleagues set up a 3D co-culture system of CAFs and tumor cells. The authors found two distinct subtypes of CAFs, one located closer to the cancer cells, which exhibited inflammatory and immune-suppression features, and another one more distant, with a myofibroblast-like phenotype supporting tumor growth. This work changes the classical view of the TME, proposing a more precise therapy to eradicate only a specific sub-population of stromal cells [10].

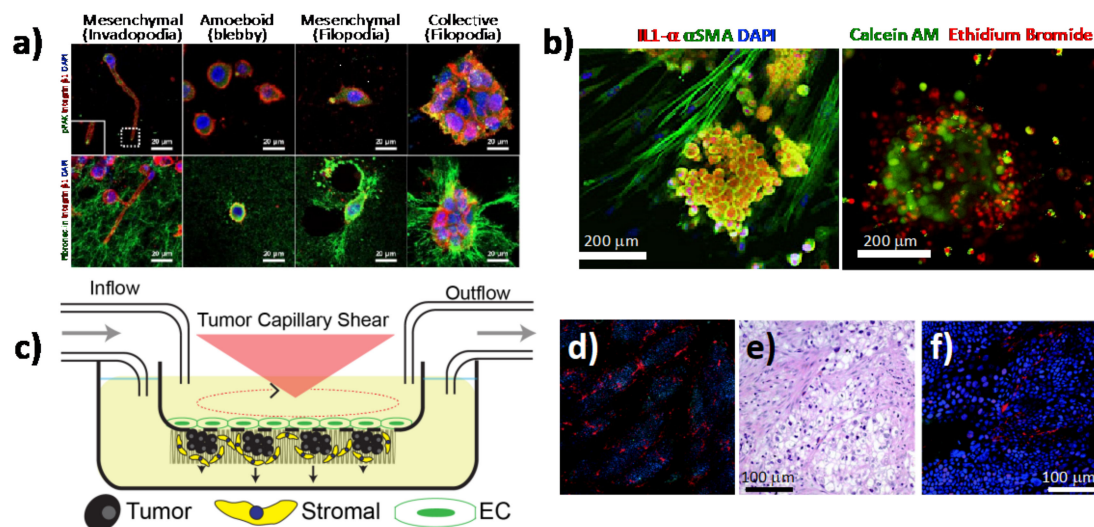


Figure 2. Heterotypic 3D in vitro models of pancreatic cancer. (a) Plasticity and mechanoreciprocity in pancreatic cancer (PC) cell migration and cell–extracellular matrix (ECM) interactions. Cancer cells showed individual or collective cell migration in 3D ECM environments. Individual PANC-1 cells formed actin-rich protrusions on the plasma membrane (invadopodia). PANC-1 cells showed organized ECM fibers along the direction of invadopodium growth. Individual BxPC-3 cells appeared as either a rounded shape (amoeboid) without podium formation or as a mesenchymal shape with actin-spike protrusions (filopodia). The mechanoreciprocity of cell–ECM interactions appeared to be associated with integrin-based adhesion. BxPC-3 cells showed extensive ECM deformation and unfolding around the filopodia along with a FAK-mediated traction force (adapted from [51]). (b) Photodestruction of fibroblasts correlates with enhanced tumor response to photodynamic therapy (PDT) using verteporfin (adapted from [53]). (c) Schematic of 3D in vitro tumor microenvironment system. Endothelial cells are plated above the transwell, and pancreatic stellate cells (PSCs) and PDAC cells are plated below the transwell. Tumor-derived hemodynamic force is applied above the transwell to the endothelial cells through rotation of the cone. The upper and lower chambers are independently perfused with media to recapitulate interstitial flow. (d) Immunofluorescence of PDAC cells (green, anti-cytokeratin 18) and PSCs (red, anti-fibroblast), nuclei stained with 4',6-diamidino-2-phenylindole DAPI. 4x composite image. (e) Immunohistochemistry (IHC) of a PDAC clinical sample. (f) Immunofluorescence stained as in the left panel (adapted from [54]).

3.3. 3D suspension Bioreactors

While not as common as the above-described 3D spheroid cultures or PDOs, 3D suspension bioreactor culture systems represent alternative models that may better mimic

the unique physiological conditions of tumors (e.g., shear forces and addition of multiple cell types). For example, bioreactors can overcome the de-differentiation and loss of specialized cellular functions, which occurs when cells are removed from their host tissue and grown as monolayers. Several bioreactor platforms exist, including the rotating wall vessel (RWV), bioreactor cartridges, or spinner flask bioreactors, each presenting unique advantages. For example, RWVs offer an optimized suspension culture by providing a low-shear, low-turbulence environment that minimizes mechanical cell damage [60], as its horizontally rotating cylindrical vessel reduces shear and turbulence associated with conventional stirred bioreactors [61]. Nonetheless, RWVs have not been as widely used for PC compared to other bioreactor platforms. For example, Brancato and co-workers applied a tissue engineering approach to produce human PDAC microtissues by co-culturing PC cells (PT45) and normal fibroblasts or CAFs within biodegradable microcarriers in a spinner flask bioreactor (Figure 3a) [62]. Morphological and histological analyses showed that the presence of fibroblasts resulted in the deposition of a stromal matrix rich in collagen, leading to the formation of tumor microtissues composed of a heterotypic cell population embedded in their own ECM (Figure 3b-d). In a different approach, Kirstein et al. developed a bioreactor cartridge-based 3D PC cell system with the ability to infuse chemotherapies at concentrations similar to those found in biological samples, such as human plasma. The authors showed that this platform was useful for assessing the role of drug pharmacokinetics and delivery optimization of anticancer treatments, such as gemcitabine [63]. Similarly, Candini et al. recently described a flat, handheld, and versatile 3D cell culture bioreactor in which the PC cell line BxPC3 could be cultured, monitored in real time, and used in 3D cytotoxicity assays [64]. The PetakaG3 LOT cell culture bioreactors, which are self-regulated, self-contained cell culture bioreactors that control oxygen, CO₂, pH, and evaporation, have also been tested for delivery of chemotherapeutics to PC cells under conditions of hypoxia [65]. While bioreactors undoubtedly possess unique advantages, they have yet to become common alternative in vitro models for PC drug discovery.

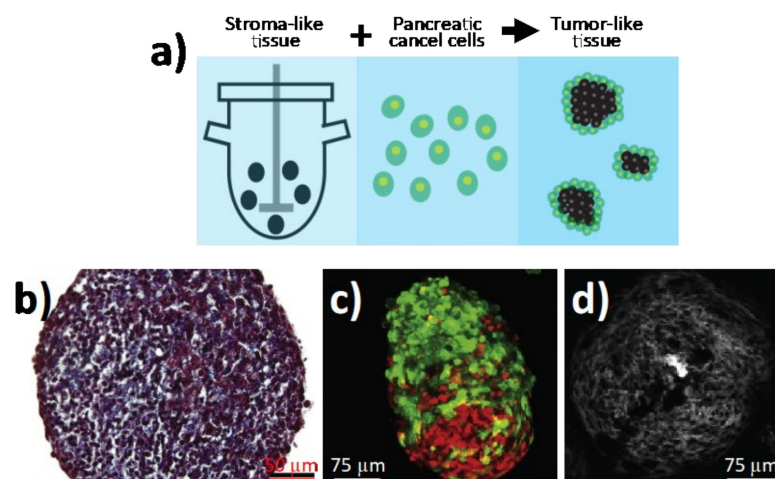


Figure 3. Bioengineered tumoral microtissues recapitulate desmoplastic reaction. (a) Schematic representation of the approach used for developing 3D in vitro PDAC bioreactor models. Stromal microtissues are produced by co-culturing normal fibroblasts or cancer-associated fibroblasts (CAFs) with gelatin microscavfold in a spinner bioreactor. After 6 days, PC cells (PT45) are added and the culture is stopped at day 12 for collecting PDAC microtissues in order to perform further investigations. (b) Masson's trichrome staining and (c) confocal imaging for CAF/PT45 microtissues at day 12 of culture. (d) Second harmonic generation signal (gray scale) from newly formed fibrillar collagen in CAF/PT45 microtissues (adapted from [62]).

4. Investigating Cell–Cell Interactions in In Vitro 3D Models

4.1. 3D Bioprinting

The use of scaffolds to generate 3D models has opened the way for innovative techniques such as 3D bioprinting. Cell printing combines scaffolds and different cell types to create a complex model with precise structure and high reproducibility [66]. Bioprinting facilitates a controlled spatial and temporal distribution of cells [67]. A 3D bioprinted tumor model can be generated by different techniques: inkjet printing, extrusion-based printing (EBP), laser-assisted bioprinting (LAB), and stereolithography [68]. 3D bioprinting has recently been used by Langer et al. to form multicellular structures consisting first of a PDAC cell core surrounded by primary human PSCs and umbilical vein endothelial cells (HUVECs). The authors demonstrated that multi-cell-type bioprinted tissues can recapitulate aspects of the in vivo tumor and provide a tunable system for the examination of several tumorigenic endpoints in the distinct tumor microenvironments [68]. Hakobyan et al. established a spheroid-based array using 3D bioprinting technology capable of reproducing the different stages of PDAC development in order to improve the understanding of PC tumor biology. This model allowed them to induce in vitro acinar to ductal cell transdifferentiation, a crucial process in PDAC progression [69].

Nevertheless, one of the major limitations of these 3D models is the lack of vasculature, which not only provides a supply of oxygen and nutrients but is essential for cancer metastasis. To overcome this limitation, microfluidics has emerged as a cutting-edge technology for combining the cellular reproducibility of PDOs with the flow control of a tumor-on-a-chip platform [57].

4.2. Organ-on-A-Chip

Although it is clear that tumors are heterogeneous mixtures of cells and ECM components, the extent to which different cell types influence cell–cell interactions as well as the paracrine signaling that is generated during therapy remains poorly understood. Nowadays, numerous microscopy-based imaging techniques are available to analyze cell morphology and cell–cell interactions within in vitro tumor models, including confocal microscopy, two-photon microscopy, and light sheet fluorescence microscopy [70–72]. One of the main advantages of using microscopy-based imaging approaches is the ability to observe spatial relations among different cell types with high temporal resolution under physiological conditions [73]. In this scenario, in vitro PDAC-on-a-chip provides powerful platforms to study the microenvironment of PDAC since these devices allow imaging of cell–cell interactions, such as tumor–endothelial and tumor–immune cell interactions, as well as cell morphological changes, by applying different types of fluorescence microscopy techniques [4,74–78]. In a recent work by Hye-ran Moon et al., a microfluidic pancreatic tumor model was developed, recapitulating the heterogeneous driver mutations of human PCs by using PDAC cells derived from genetically engineered mouse models (KPC with *Kras* and *Trp53* mutations, and KIC with *Kras* mutation and *Cdkn2a* deletion) in order to mimic the intra-tumoral heterogeneity (Figure 4a) [77]. The model was successfully used to study interaction mechanisms between heterogeneous cancer cell subpopulations exposed to anti-cancer drugs and associated drug resistance. By means of fluorescence microscopy, the authors observed significant morphological changes in the epithelial phenotype KIC (eKIC) cells co-cultured with the mesenchymal phenotype KIC (mKIC) cells at the level of enhanced gemcitabine resistance in the co-culture models (Figure 4b), suggesting that interactions between these two cancer cell types induced multiple changes of the eKIC cells including loss of epithelial characteristics, most likely causing increased resistance to gemcitabine. By means of confocal immunofluorescence, the authors assessed the changes in E-cadherin (E-cad) expression and observed that when co-culturing cells, E-cad expression in eKIC was significantly reduced, implying that the interactions between heterogeneous cancer cells may induce the phenotype transition of epithelial cancer cell types. In a different approach, Nguyen and colleagues reported a new organotypic PDAC-on-a-chip model that mimics vascular invasion and tumor–blood vessel interactions

(Figure 4c–f) [79]. The microfluidic device is composed of two hollow cylindrical channels embedded within a 3D collagen matrix. One channel is seeded with endothelial cells to form a perfusable biomimetic blood vessel, while the other channel is seeded with PC cells to form a pancreatic cancer duct. To study the interactions of PDAC cells with the blood vessels, the authors performed a screening experiment wherein different chemotactic agents were introduced into the biomimetic blood vessel and found that a gradient of fetal bovine serum most efficiently stimulated the invasion of PC cells into the collagen matrix. By means of confocal microscopy, the authors were able to record the ablation of blood vessel by cancer cells—notably, they observed that once in contact with the biomimetic blood vessel, the PDAC cells wrapped around the blood vessel and spread along the length of the blood vessel before invading into the vessel itself, leaving behind tumor-lined and tumor-filled luminal structures (Figure 4c–f). The infiltration of immunosuppressive cells is critical in the generation and maintenance of an immunosuppressive environment in PDAC, thus contributing to the failure of current available therapeutic approaches. In this regard, cell–cell interaction studies have revealed an important interplay between tumor-associated macrophages and regulatory T cells (Tregs). By using light sheet fluorescent microscopy, Siret C. et al. were able to show a direct interaction between myeloid-derived suppressor cells (MDSCs) and Tregs cells in a 3D PDAC tumor context [80]. These findings were also corroborated by the use of the transwell system, which demonstrated that cell-to-cell interactions are required for Treg cell proliferation and development induced by MDSCs. However, Treg cells were also shown to modulate proliferation and survival of MDSCs. Remarkably, by coupling imaging approaches and functional assays, the authors were able to show that physical interactions between cells contribute to the establishment of an immunosuppressive environment in PDAC.

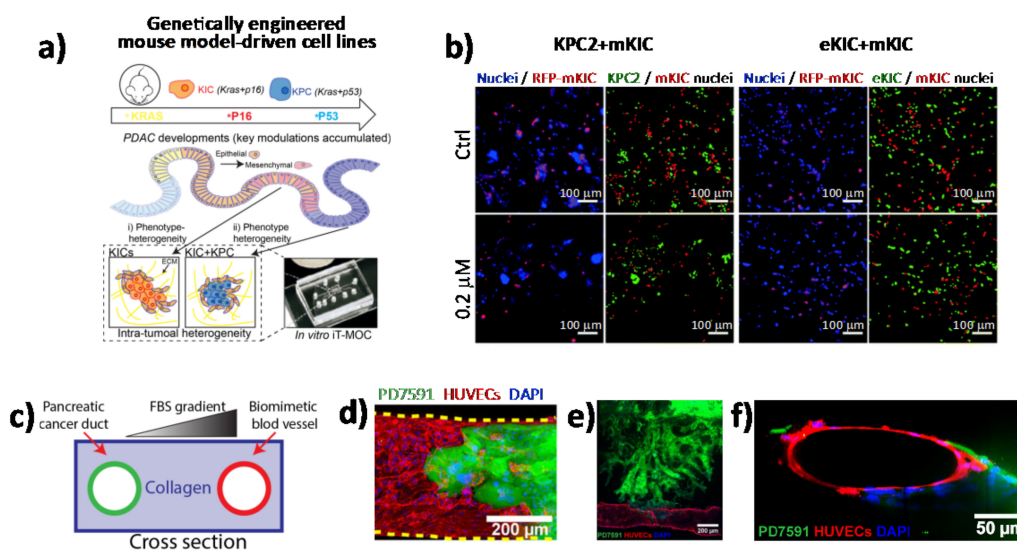


Figure 4. Direct imaging of cell–cell interactions in 3D in vitro models of PC. (a) Schematic illustration of the functional model of the in vitro intra-tumoral heterogeneous features composed by genetically engineered mouse model-driven cell lines to capture different PDAC progression stages. (b) Representative fluorescent micrographs of co-cultured KPC2–mKIC and eKIC–mKIC in control (Ctrl), 0.2 μM, and 20 μM gemcitabine treatment groups. Nuclei (blue) of each cell are distinguished in green (KPC2 and eKIC) and red (mKIC). Abbreviations: iT-MOC (interstitial tumor-microenvironment-on-a-chip), KIC genotypes (Kras mutation and Cdkn2a deletion), mKIC (mesenchymal phenotype KIC), murine pancreatic cancer cell lines (KPC2, eKIC, and mKIC). (a,b) (adapted from [77]). (c) Schematic illustration of PDAC-on-a-chip with a biomimetic blood vessel and a PC duct. One channel is seeded with endothelial cells to form a perfusable biomimetic blood vessel, while the other channel is seeded with PC cells to form a tumor duct. FBS (fetal bovine serum). (d) Representative confocal image of a section of the blood vessel (in red) invaded by YFP PD7591 PDAC cell (in green), showing that part of the blood vessel is being ablated by cancer cells in the organotypic model. (e) YFP PD7591 cells (in green) invading the biomimetic blood vessel (in red), migrating along the vessel and wrapping around the blood vessel. (f) Cross-sectional image of the biomimetic blood vessel shown in (e). (c–e) (adapted from [79]).

5. The End of Perpetual Chemotherapy: Nanoparticles (NPs) for Cell Targeting

For decades, gemcitabine (Gem)-based therapy has been the first-line treatment for patients with PC with an overall improvement in survival of only 6 months, where surgery is not an option [81]. Most recently, FOLFIRINOX (consisting of oxaliplatin, irinotecan, fluorouracil, and leucovorin) has achieved a slight increase in patient survival compared with Gem alone; however, it is associated with numerous side effects, including diarrhea, anemia, and increased risk of infections [82]. The presence of a dense desmoplastic stroma within PDAC tumors is the principle cause of chemotherapy failure, since it leads to an increased interstitial fluid pressure (IFP), which implies hypovascularity, reduced tumor perfusion, and the generation of a hypoxic environment [83]. Therefore, the stroma acts as a physical and biological barrier that inhibits drug delivery, thus contributing to therapy resistance [84]. In this scenario, nanomedicine has changed the world of cancer therapy. Nano-sized vehicles encapsulating drugs exhibit greater cellular uptake and prolonged circulation compared to classical chemotherapy. They possess the capability to overcome biological barriers, protect drugs from degradation, and foster their accumulation at the target site, and they are associated with reduced side effects [85,86]. Nanocarriers have been developed on the basis of natural (e.g., lipid, polyethylene glycol, poly(lactide-*o*-glycolic) acid, and chitosan) polymers or inorganic nanoparticles (e.g., gold, magnetic, mesoporous silica, and quantum dots) [87,88]. The first two FDA-approved nanomolecules for PDAC treatment were Abraxane, an albumin-bound paclitaxel-containing nanoparticle (NP), and Onivyde, an irinotecan liposome-based injection, which induced an increase in patient survival of 2-4 months compared to frontline treatment [89,90]. At the same time, strategies aimed at the disruption of stromal barriers to improve drug delivery have been explored with slight success [91]. Caution must be taken at the level of eliminating the stroma barrier (i.e., CAFs), as was exemplified by the failure of the Infinity Pharmaceuticals trial using IPI-926-03, a drug that depletes tumor-associated stromal tissue by inhibition of the HH cellular signaling pathway. Specifically, the trial was halted after patients in the gemcitabine + IPI-926 arm showed reduced overall survival compared to gemcitabine alone. Nonetheless, since this trial, new studies using, for example, vismodegib (formerly known as GDC-0449) have confirmed therapeutic effectiveness and response and have been evaluated in multiple clinical trials with other tumor entities (ClinicalTrials.gov Identifier: NCT02465060). The majority of nanoparticles have been designed for a controlled cargo release in response to distinct endogenous/exogenous stimuli such as pH level [92], temperature [93], redox reactions [94], enzyme activity [95], magnetic/electric field [96], mechanical force, and ultrasound/light irradiation [97]. Most recently, a new class of theranostic NPs have emerged, which enable simultaneous diagnosis, targeted delivery, and monitoring of therapy response [98,99]. Rosenberger et al. co-encapsulated the magnetic iron oxide NPs (IONPs) and the fluorescein isothiocyanate (FITC) dye within hyaluronic acid (HA)-functionalized NPs. This system takes advantage of the specific recognition of HA by the CD44 receptor (highly expressed on PDAC cells) and combines magnetic resonance with fluorescence imaging [100]. PC is considered a “cold tumor” with limited antigenic expression, making this tumor less likely to respond to immunotherapy. Several efforts have been evaluated, such as using PDT, chemotherapy, and other strategies to make PC more immunogenic [101]. In the last decades, tumor immunotherapy has emerged as a promising alternative to chemotherapy, but the inherent immune-suppressive pancreatic TME represents a challenge for its success. The use of specific NPs to activate the immune system within the TME is evolving as an efficient strategy to improve immunotherapy efficacy [102,103]. In this regard, one of the most promising approaches consists in targeting the interaction between the programmed death ligand 1 (PD-L1) with its receptor (PD-1), expressed by T lymphocytes. The PD-L1 protein is present on the surface of several cancer cells and its binding with PD-1 inhibits the activation of T cells, thus suppressing the immune response [104]. Mia and colleagues formulated a lipid-based (LPD) nanocarrier embedding a plasmid encoding for a fusion protein (called trap), specifically binding CXCL12 and PD-L1 for targeting PC [105]. The LPD nanocarriers were injected into mice

bearing orthotopic PC tumors and were found to bind CXCL12, thus facilitating CD3⁺T-cell infiltration into the tumor. This therapy significantly reduced metastasis through the stimulation of the immunosuppressive TME. It is known that indoleamine 2,3-dioxygenase (IDO) enzyme, frequently overexpressed in tumors, contributes to the immunosuppressive microenvironment of cancer cells by suppressing the T cell proliferation through the depletion of tryptophan [106]. Lu and colleagues induced the suppression of the IDO pathway with the induction of immunogenic cell death (ICD) by using mesoporous silica nanoparticles (MSNPs) encapsulating the IDO inhibitor together with oxaliplatin. This system allowed for the recruitment of cytotoxic T lymphocytes and the downregulation of Foxp3⁺ T cells *in vivo*, leading to the reduction of tumor volume [107]. In addition to drug release, NPs can also encapsulate small RNA molecules, alone or with drugs, to silence cancer-causing genes and suppress tumor growth [108]. All these different approaches can be improved with the surface-functionalization of NPs with specific tumor-targeting ligands or antibodies for site-specific drug delivery [109]. NPs can have precise light interaction characteristics, making them suitable for several detection techniques, such as magnetic resonance imaging [110], Raman/SERS (Surface Enhanced Raman Spectroscopy) spectroscopy [111,112], two-photon microscopy [113], and photoacoustic analysis [114]. However, few of these techniques have been applied in 3D cancer models. Lazzari and colleagues tracked a doxorubicin-loaded polymeric NP diffusion in a complex PC 3D model (composed by cancer, endothelial, and fibroblast cells) using confocal laser scanning microscopy (CLSM). Their results clearly showed that CLSM was not suitable to accurately monitor the diffusion of small molecules such as doxorubicin due to the progressive loss of their fluorescence signal [115] (Figure 5a). Because complex 3D cancer models are designed to resemble the *in vivo* environment with low pH, the drugs/fluorescent dyes could detach from the surface of NPs before entering cells. Recently, Darrigues et al. generated spheroids by co-culturing PC cells and PSCs in various ratios to mimic different tumor–stromal compositions and to explore NP penetration. The authors used fluorescence live imaging, photothermal analysis, and photoacoustic analysis to observe nanoparticle performance in the spheroids, finding that the nanorods enabled multi-imaging detection even when fluorescence tracking was not possible [116] (Figure 5b). Despite the possible drawbacks, 3D models are still superb tools for understanding how multi-functional NPs interact with the *in vivo* environment.

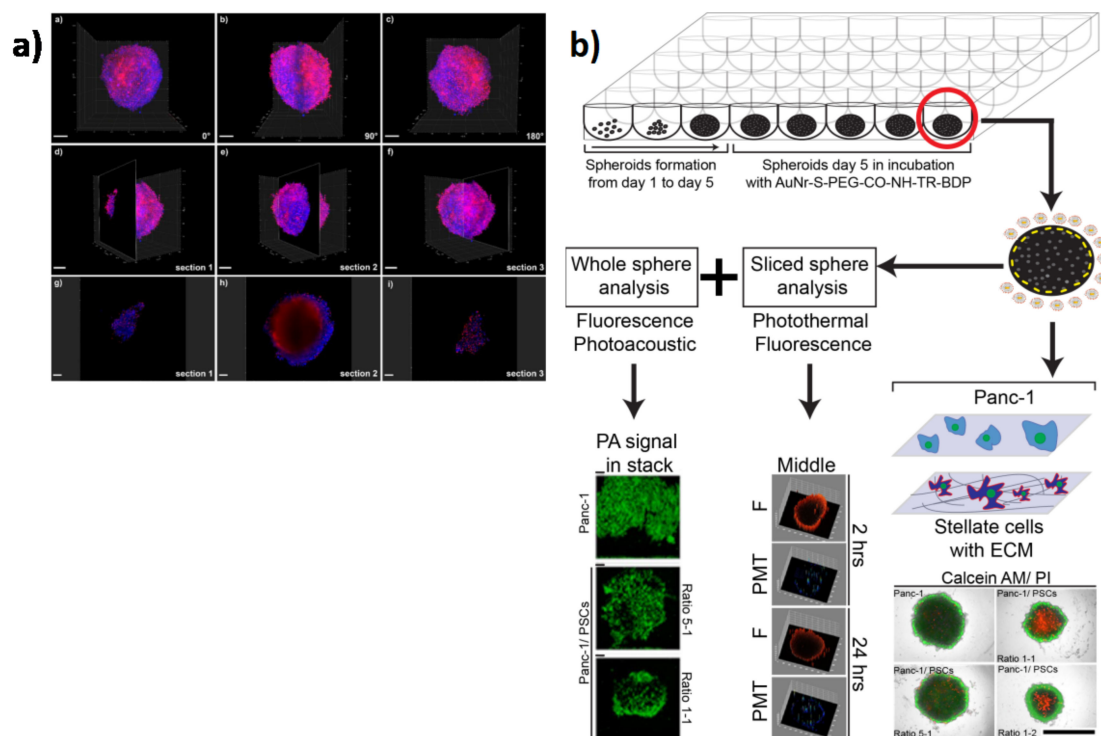


Figure 5. Nanoparticle applications in 3D in vitro models of PC. (a) 3D tomography with light sheet fluorescence microscopy of large hetero-type multicellular tumor spheroids after incubation with doxorubicin (Dox). Overlays of blue (nuclei, Hoechst 33342 staining) and red (Dox) channels. (a) 0° rotation, (b) 90° rotation, and (c) 180° rotation. Localization of (d) section 1 (113 μm depth), (e) section 2 (403 μm depth), and (f) section 3 (861 μm depth) in relation to the entire spheroid. Scale bars: 200 μm . Images taken at (g) section 1, (h) section 2, and (i) section 3. Scale bars: 100 μm (adapted from [115]). (b) Schematic of the experimental approach: spheroid formation (day 1 to day 5) in ultra-low-attachment 96-well plate, functionalized gold nanodot (AuNR) incubation, followed by characterization of the whole sphere and a section of it (adapted from [116]).

6. Conclusions

It is widely recognized that spatial and temporal cell–cell communications in the microenvironment contributes to PC initiation and progression. To study the complex cell–cell interactions, researchers must implement innovative experimental and analytical strategies. Recently, the development of in vitro 3D patient-derived cancer models has emerged as a revolutionary approach for effective in vitro anticancer drug screening. Furthermore, next-generation platforms of anticancer drugs, including nanoparticle-based delivery agents, will focus on the malignant phenotype as a whole and not just on cell proliferation. Thus, 3D cancer models provide an exceptional platform for studying critical cancer events not obtainable with other models. For instance, xenograft models resemble the original tissue but are expensive, time-consuming, and not suitable for high-throughput drug screening. Another promising avenue is the creation of tumor-on-a-chip platforms. This technology allows for reconstructing the cancer complexity with a dynamic physical microenvironment and, by linking different physiological modules, including vasculature, can be used to investigate the interactions between cancer and other organs. Certainly, all these models have several advantages and disadvantages, and there is no single method that satisfies all research needs. For this reason, further studies are required for the development of innovative in vitro pre-clinical models that can better overcome the limitations of these systems, leading to an improvement in personalized medicine (Figure 6 and Table 1). The use of in vitro 3D tumor models coupled with advanced high throughput and automated imaging techniques remains a promising direction for accelerating translation of these 3D cancer cultures into clinically relevant models for personalized medicine in the treatment of PC.

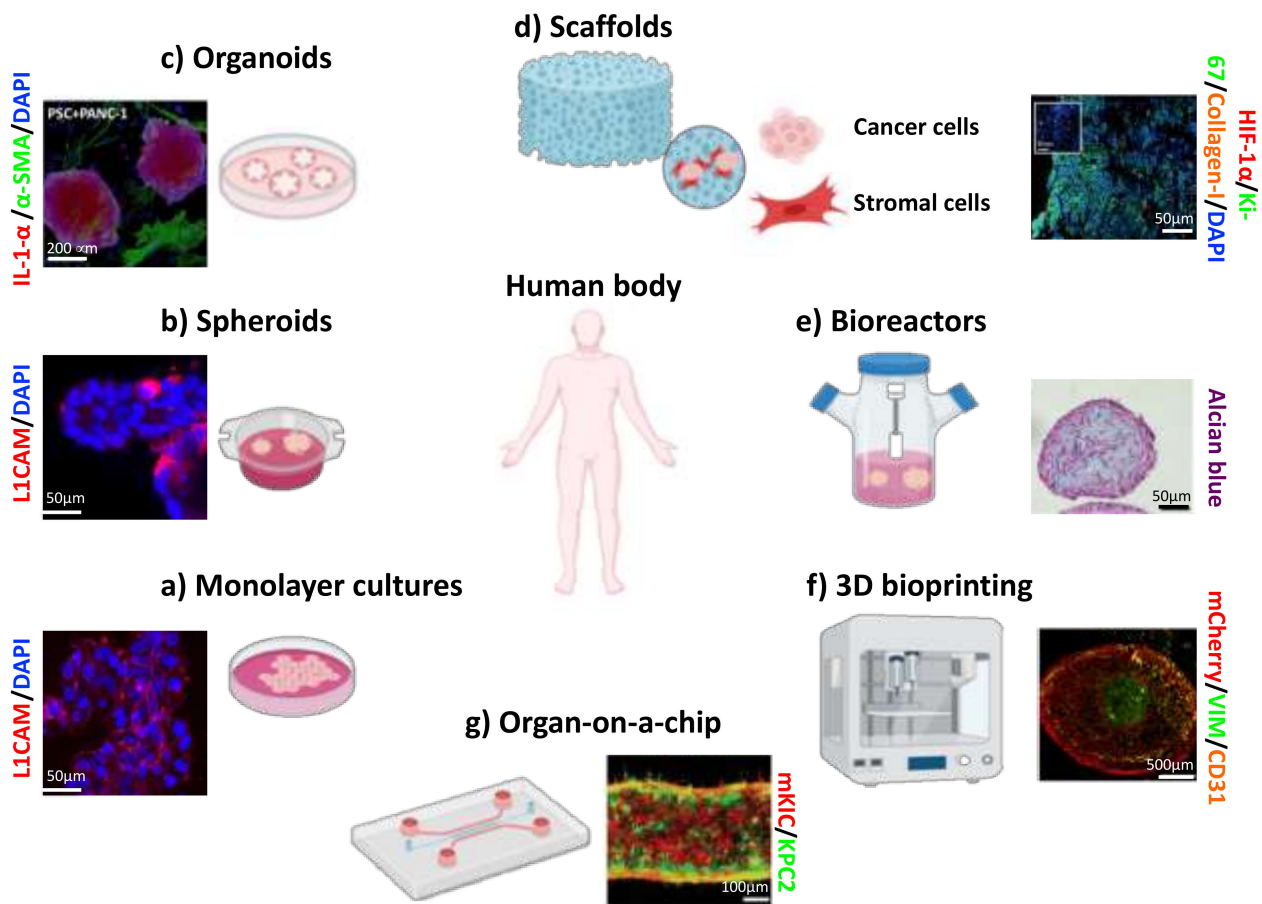


Figure 6. The evolving strategies for culturing and studying PC cells from human tissues. Representative immunofluorescence images of L3.6pl PDAC cells grown as monolayers (a) or spheroids (b) (adapted from [34]). (c) 3D confocal image of organoids generated by co-culturing PSCs (green) with PANC-1 (red) cells (adapted from [53]). (d) Fluorescent image of PANC-1 cells co-cultured with stromal cells on collagen-I scaffold (adapted from [42]). (e) Detection of glycosaminoglycans by Alcian blue staining in a homotypic 3D bio-reactor culture of human CAFs generated by bioengineered tumoral microtissues (adapted from [62]). (f) Representative immunofluorescence image of 3D bioprinted tissues for PDAC (green), PSC (red), and endothelial (yellow) cells (adapted from [68]). (g) IF image of the invasion of a heterogeneous co-culture of PDAC cells (adapted from [75]).

Table 1. Advantages and disadvantages of in vitro 3D culture models.

Technique	Advantages	Disadvantages
Monolayer cultures a	<ul style="list-style-type: none"> Cost effective Easy-to-use protocol Scalable to different plate formats Compliant with high-throughput screening (HTS) High reproducibility Formed from primary cells and cell lines 	<ul style="list-style-type: none"> Shape changed from original tissue (polarization lost) Lack vasculature Reduces cell-to-cell interactions Less biologically relevant models
Spheroids	<ul style="list-style-type: none"> Easy-to-use protocol Scalable to different plate formats Compliant with high-throughput screening (HTS) Formed from primary cells and cell lines Long-term culture Allows co-cultures 	<ul style="list-style-type: none"> Simple architectures Cannot control uniformity (size, composition) Not all cell lines form spheroids Agglomeration Necrotic cores Lack vasculature

Table 1. Cont.

Technique	Advantages	Disadvantages
Organoids	Patient-specific Scalable to different plate formats Formed from primary cells Allows co-cultures In vivo-like complexity In vivo-like architecture Amenable for tissue engineering and transplantation	Costly Not easy-to-use protocol Cannot control uniformity (size, composition) Less amenable to HTS May lack key cell types Lack vasculature Require validation to identify outgrowth of unwanted cells Requires access to human samples
Scaffolds	Scalable to different plate formats Compliant with high-throughput screening (HTS) High reproducibility Formed from primary cells and cell lines Long term culture Allows co-cultures In vivo-like complexity In vivo-like architecture Amenable for tissue engineering and transplantation Naturally-derived ECM components of synthetic polymers Resemble mechanical forces in tumors Versatile Tunable composition	Costly Not easy-to-use protocol Simple architectures Batch-to-batch variability of natural matrixes Might require complex cell retrieval/imaging methods
Bioreactors	High density cell expansion Controllable culture parameters	Costly Requires optimization of cell parameters and biomaterial inclusion Hydrodynamic shear stress
Organ-on-a-chip	Compliant with high-throughput screening (HTS) High reproducibility Formed from primary cells and cell lines Allow co-cultures In vivo-like complexity In vivo-like architecture Controllable culture parameters Vascularized	Costly Requires special equipment Difficult to scale up
3D Bioprinting	High-throughput production High reproducibility Formed from primary cells and cell lines Allow co-cultures In vivo-like complexity In vivo-like architecture Controllable culture parameters Vascularized	Costly Requires special equipment Challenges with cells/materials Issues with tissue maturation Needs optimization

Author Contributions: Writing—original draft preparation, D.D.C, R.R., L.L.d.M., and E.L.; writing—review and editing, L.L.d.M., B.S.J., and E.L.; supervision, E.L.; funding acquisition, L.L.d.M., G.G., B.S.J. and E.L. All authors have read and agreed to the published version of the manuscript.

Funding: My First AIRC Grant (MFAG-2017, #20206) and POR Campania FESR 2014/2020 (Project SATIN) to E.L., L.L.d.M. gratefully acknowledges support from the European Research Council (ERC) under the European Union’s Horizon 2020 research and innovation program ERC Starting Grant “INTERCELLMED” (grant agreement no. 759959) and the project “Tecnapolo per la medicina di precisione” (TecnoMed Puglia) Regione Puglia: DGR n.2117 of 21/11/2018, CUP: B84I18000540002. B.S.

acknowledges support from a EuroNanoMed III 2018 project “PANIPAC” co-financed by the Spanish Ministry of Science and Innovation (PCI2019-103725).

Acknowledgments: We would like to thank all the members of the laboratory of E.L. for fruitful discussions.

Conflicts of Interest: The authors declare no conflict of interest for this article.

References

1. Fitzmaurice, C. Global Burden of Disease Cancer Collaboration. Global, regional, and national cancer incidence, mortality, years of life lost, years lived with disability, and disability-adjusted life-years for 29 cancer groups, 2006 to 2016: A systematic analysis for the Global Burden of Disease study. *J. Clin. Oncol.* **2018**, *36*, 1568. [[CrossRef](#)]
2. Rahib, L.; Smith, B.D.; Aizenberg, R.; Rosenzweig, A.B.; Fleshman, J.M.; Matrisian, L.M. Projecting cancer incidence and deaths to 2030: The unexpected burden of thyroid, liver, and pancreas cancers in the United States. *Cancer Res.* **2014**, *74*, 2913–2921. [[CrossRef](#)] [[PubMed](#)]
3. Silvestris, N.; Brunetti, O.; Bittoni, A.; Cataldo, L.; Corsi, D.; Crippa, S.; D’Onofrio, M.; Fiore, M.; Giommoni, E.; Milella, M.; et al. Clinical Practice Guidelines for Diagnosis, Treatment and Follow-up of Exocrine Pancreatic Ductal Adenocarcinoma: Evidence Evaluation and Recommendations by the Italian Association of Medical Oncology (AIOM). *Cancers* **2020**, *12*, 1681. [[CrossRef](#)]
4. Swayden, M.; Soubeyran, P.; Iovanna, J. Upcoming Revolutionary Paths in Preclinical Modeling of Pancreatic Adenocarcinoma. *Front. Oncol.* **2020**, *9*, 1443. [[CrossRef](#)]
5. Michalski, C.W.; Rosendahl, J.; Michl, P.; Kleeff, J. Translational Pancreatic Cancer Research: From Understanding of Mechanisms to Novel Clinical Trials. In *Molecular and Translational Medicine*; Springer International Publishing: Cham, Switzerland, 2020; ISBN 978-3-030-49475-9.
6. Ben-David, U.; Ha, G.; Tseng, Y.-Y.; Greenwald, N.F.; Oh, C.; Shih, J.; McFarland, J.M.; Wong, B.; Boehm, J.S.; Beroukhi, R.; et al. Patient-Derived Xenografts Undergo Murine-Specific Tumor Evolution. *Nat. Genet.* **2017**, *49*, 1567. [[CrossRef](#)] [[PubMed](#)]
7. Barros, A.S.; Costa, E.C.; Nunes, A.S.; De Melo-Diogo, D.; Correia, I.J. Comparative study of the therapeutic effect of Doxorubicin and Resveratrol combination on 2D and 3D (spheroids) cell culture models. *Int. J. Pharm.* **2018**, *551*, 76–83. [[CrossRef](#)]
8. Thomas, D.; Radhakrishnan, P. Tumor-stromal crosstalk in pancreatic cancer and tissue fibrosis. *Mol. Cancer* **2019**, *18*, 1–15. [[CrossRef](#)]
9. Dougan, S.K. The Pancreatic Cancer Microenvironment. *Cancer J.* **2017**, *23*, 321–325. [[CrossRef](#)] [[PubMed](#)]
10. Öhlund, D.; Handy-Santana, A.; Biffi, G.; Elyada, E.; Almeida, A.S.; Ponz-Sarvisse, M.; Corbo, V.; Oni, T.E.; Hearn, S.A.; Lee, E.J.; et al. Distinct populations of inflammatory fibroblasts and myofibroblasts in pancreatic cancer. *J. Exp. Med.* **2017**, *214*, 579–596. [[CrossRef](#)]
11. Westphalen, C.B.; Olive, K.P. Genetically Engineered Mouse Models of Pancreatic Cancer. *Cancer J.* **2012**, *18*, 502–510. [[CrossRef](#)]
12. Gopinathan, A.; Morton, J.P.; Jodrell, D.I.; Sansom, O.J. GEMMs as preclinical models for testing pancreatic cancer therapies. *Dis. Model. Mech.* **2015**, *8*, 1185–1200. [[CrossRef](#)] [[PubMed](#)]
13. Tomás-Bort, E.; Kieler, M.; Sharma, S.; Candido, J.B.; Loessner, D. 3D approaches to model the tumor microenvironment of pancreatic cancer. *Theranostics* **2020**, *10*, 5074–5089. [[CrossRef](#)]
14. Ehlen, L.; Arndt, J.; Treue, D.; Bischoff, P.; Loch, F.N.; Hahn, E.M.; Kotsch, K.; Klauschen, F.; Beyer, K.; Margonis, G.A.; et al. Novel methods for in vitro modeling of pancreatic cancer reveal important aspects for successful primary cell culture. *BMC Cancer* **2020**, *20*, 1–13. [[CrossRef](#)] [[PubMed](#)]
15. Cavo, M.; Serio, F.; Kale, N.R.; D’Amone, E.; Gigli, G.; Del Mercato, L.L. Electrospun nanofibers in cancer research: From engineering of in vitro 3D cancer models to therapy. *Biomater. Sci.* **2020**, *8*, 4887–4905. [[CrossRef](#)] [[PubMed](#)]
16. Polini, A.; Del Mercato, L.L.; Barra, A.; Zhang, Y.S.; Calabi, F.; Gigli, G. Towards the development of human immune-system-on-a-chip platforms. *Drug Discov. Today* **2019**, *24*, 517–525. [[CrossRef](#)]
17. Turetta, M.; Del Ben, F.; Brisotto, G.; Biscontin, E.; Bulfoni, M.; Cesselli, D.; Colombatti, A.; Scoles, G.; Gigli, G.; Del Mercato, L.L. Emerging Technologies for Cancer Research: Towards Personalized Medicine with Microfluidic Platforms and 3D Tumor Models. *Curr. Med. Chem.* **2018**, *25*, 4616–4637. [[CrossRef](#)]
18. Kimlin, L.; Kassis, J.; Virador, V. 3D in vitro tissue models and their potential for drug screening. *Expert Opin. Drug Discov.* **2013**, *8*, 1455–1466. [[CrossRef](#)]
19. Longati, P.; Jia, X.; Eimer, J.; Wagman, A.; Witt, M.-R.; Rehnmark, S.; Verbeke, C.; Toftgård, R.; Löhr, M.; Heuchel, R.L. 3D pancreatic carcinoma spheroids induce a matrix-rich, chemoresistant phenotype offering a better model for drug testing. *BMC Cancer* **2013**, *13*, 95. [[CrossRef](#)]
20. Langhans, S.A. Three-Dimensional in Vitro Cell Culture Models in Drug Discovery and Drug Repositioning. *Front. Pharmacol.* **2018**, *9*, 6. [[CrossRef](#)] [[PubMed](#)]
21. Cavo, M.; Cave, D.D.; D’Amone, E.; Gigli, G.; Lonardo, E.; Del Mercato, L.L. A synergic approach to enhance long-term culture and manipulation of MiaPaCa-2 pancreatic cancer spheroids. *Sci. Rep.* **2020**, *10*, 1–11. [[CrossRef](#)]
22. Zeeberg, K.; Cardone, R.A.; Greco, M.R.; Saccomano, M.; Nøhr-Nielsen, A.; Alves, F.; Pedersen, S.F.; Reshkin, S.J. Assessment of different 3D culture systems to study tumor phenotype and chemosensitivity in pancreatic ductal adenocarcinoma. *Int. J. Oncol.* **2016**, *49*, 243–252. [[CrossRef](#)] [[PubMed](#)]

23. Boj, S.F.; Hwang, C.-I.; Baker, L.A.; Chio, I.I.C.; Engle, D.D.; Corbo, V.; Jager, M.; Ponz-Sarvisé, M.; Tiriác, H.; Spector, M.S.; et al. Organoid models of human and mouse ductal pancreatic cancer. *Cell* **2015**, *160*, 324–338. [[CrossRef](#)] [[PubMed](#)]
24. Hwang, C.-I.; Boj, S.F.; Clevers, H.; Tuveson, D.A. Preclinical models of pancreatic ductal adenocarcinoma. *J. Pathol.* **2016**, *238*, 197–204. [[CrossRef](#)]
25. Moreira, L.; Bakir, B.; Chatterji, P.; Dantes, Z.; Reichert, M.; Rustgi, A.K. Pancreas 3D Organoids: Current and Future Aspects as a Research Platform for Personalized Medicine in Pancreatic Cancer. *Cell. Mol. Gastroenterol. Hepatol.* **2018**, *5*, 289–298. [[CrossRef](#)] [[PubMed](#)]
26. Fujii, M.; Clevers, H.; Sato, T. Modeling Human Digestive Diseases with CRISPR-Cas9-Modified Organoids. *Gastroenterology* **2019**, *156*, 562–576. [[CrossRef](#)]
27. Tiriác, H.; Belleau, P.; Engle, D.D.; Plenker, D.; Deschênes, A.; Somerville, T.D.D.; Froeling, F.E.M.; Burkhart, R.A.; Denroche, R.E.; Jang, G.H.; et al. Organoid Profiling Identifies Common Responders to Chemotherapy in Pancreatic Cancer. *Cancer Discov.* **2018**, *8*, 1112–1129. [[CrossRef](#)]
28. Driehuis, E.; Van Hoeck, A.; Moore, K.; Kolders, S.; Francies, H.E.; Gulersonmez, M.C.; Stigter, E.C.A.; Burgering, B.; Geurts, V.; Gracanin, A.; et al. Pancreatic cancer organoids recapitulate disease and allow personalized drug screening. *Proc. Natl. Acad. Sci. USA* **2019**, *116*, 26580–26590. [[CrossRef](#)]
29. Seino, T.; Kawasaki, S.; Shimokawa, M.; Tamagawa, H.; Toshimitsu, K.; Fujii, M.; Ohta, Y.; Matano, M.; Nanki, K.; Kawasaki, K.; et al. Human Pancreatic Tumor Organoids Reveal Loss of Stem Cell Niche Factor Dependence during Disease Progression. *Cell Stem Cell* **2018**, *22*, 454–467. [[CrossRef](#)]
30. Frappart, P.; Walter, K.; Gout, J.; Beutel, A.K.; Morawe, M.; Arnold, F.; Breunig, M.; Barth, T.F.; Marienfeld, R.; Schulte, L.; et al. Pancreatic cancer-derived organoids—A disease modeling tool to predict drug response. *United Eur. Gastroenterol. J.* **2020**, *8*, 594–606. [[CrossRef](#)]
31. Nelson, S.R.; Zhang, C.; Roche, S.; O’Neill, F.; Swan, N.; Luo, Y.; Larkin, A.; Crown, J.; Walsh, N. Modelling of pancreatic cancer biology: Transcriptomic signature for 3D PDX-derived organoids and primary cell line organoid development. *Sci. Rep.* **2020**, *10*, 1–12. [[CrossRef](#)]
32. Schuster, B.; Junkin, M.; Kashaf, S.S.; Romero-Calvo, I.; Kirby, K.; Matthews, J.; Weber, C.R.; Rzhetsky, A.; White, K.P.; Tay, S. Automated microfluidic platform for dynamic and combinatorial drug screening of tumor organoids. *Nat. Commun.* **2020**, *11*, 1–12. [[CrossRef](#)]
33. Ho, W.J.; Jaffee, E.M.; Zheng, L. The tumour microenvironment in pancreatic cancer—Clinical challenges and opportunities. *Nat. Rev. Clin. Oncol.* **2020**, *17*, 527–540. [[CrossRef](#)]
34. Cave, D.D.; Di Guida, M.; Costa, V.; Sevillano, M.; Ferrante, L.; Heeschen, C.; Corona, M.; Cucciardi, A.; Lonardo, E. TGF- β 1 secreted by pancreatic stellate cells promotes stemness and tumorigenicity in pancreatic cancer cells through L1CAM downregulation. *Oncogene* **2020**, *39*, 4271–4285. [[CrossRef](#)] [[PubMed](#)]
35. Feig, C.; Gopinathan, A.; Neesse, A.; Chan, D.S.; Cook, N.; Tuveson, D.A. The Pancreas Cancer Microenvironment. *Clin. Cancer Res.* **2012**, *18*, 4266–4276. [[CrossRef](#)]
36. Padoan, A.; Plebani, M.; Basso, D. Inflammation and Pancreatic Cancer: Focus on Metabolism, Cytokines, and Immunity. *Int. J. Mol. Sci.* **2019**, *20*, 676. [[CrossRef](#)] [[PubMed](#)]
37. Puls, T.J.; Tan, X.; Whittington, C.F.; Voytik-Harbin, S.L. 3D collagen fibrillar microstructure guides pancreatic cancer cell phenotype and serves as a critical design parameter for phenotypic models of EMT. *PLoS ONE* **2017**, *12*, e0188870. [[CrossRef](#)]
38. Chiellini, F.; Puppi, D.; Piras, A.M.; Morelli, A.; Bartoli, C.; Migone, C. Modelling of pancreatic ductal adenocarcinoma in vitro with three-dimensional microstructured hydrogels. *RSC Adv.* **2016**, *6*, 54226–54235. [[CrossRef](#)]
39. Ricci, C.; Mota, C.; Moscato, S.; D’Alessandro, D.; Ugel, S.; Sartoris, S.; Bronte, V.; Boggi, U.; Campani, D.; Funel, N.; et al. Interfacing polymeric scaffolds with primary pancreatic ductal adenocarcinoma cells to develop 3D cancer models. *Biomatter* **2014**, *4*, e955386. [[CrossRef](#)]
40. Bregenzler, M.E.; Horst, E.N.; Mehta, P.; Novak, C.M.; Raghavan, S.; Snyder, C.S.; Mehta, G. Integrated cancer tissue engineering models for precision medicine. *PLoS ONE* **2019**, *14*, e0216564. [[CrossRef](#)]
41. Burdett, E.; Kasper, F.K.; Mikos, A.G.; Ludwig, J.A. Engineering Tumors: A Tissue Engineering Perspective in Cancer Biology. *Tissue Eng. Part B Rev.* **2010**, *16*, 351–359. [[CrossRef](#)] [[PubMed](#)]
42. Totti, S.; Allenby, M.C.; Dos Santos, S.B.; Mantalaris, A.; Velliou, E.G. A 3D bioinspired highly porous polymeric scaffolding system for in vitro simulation of pancreatic ductal adenocarcinoma. *RSC Adv.* **2018**, *8*, 20928–20940. [[CrossRef](#)]
43. Baker, L.A.; Tiriác, H.; Clevers, H.; Tuveson, D.A. Modeling Pancreatic Cancer with Organoids. *Trends Cancer* **2016**, *2*, 176–190. [[CrossRef](#)] [[PubMed](#)]
44. Guillaume, L.; Rigal, L.; Fehrenbach, J.; Severac, C.; Ducommun, B.; Lobjois, V. Characterization of the physical properties of tumor-derived spheroids reveals critical insights for pre-clinical studies. *Sci. Rep.* **2019**, *9*, 1–9. [[CrossRef](#)]
45. Schnittert, J.; Bansal, R.; Prakash, J. Targeting Pancreatic Stellate Cells in Cancer. *Trends Cancer* **2019**, *5*, 128–142. [[CrossRef](#)]
46. Birbrair, A. Tumor Microenvironment: Non-Hematopoietic Cells. In *Advances in Experimental Medicine and Biology*; Springer International Publishing: Cham, Switzerland, 2020; Volume 1234, ISBN 978-3-030-37183-8.
47. Lonardo, E.; Frias-Aldeguer, J.; Hermann, P.C.; Heeschen, C. Pancreatic stellate cells form a niche for cancer stem cells and promote their self-renewal and invasiveness. *Cell Cycle* **2012**, *11*, 1282–1290. [[CrossRef](#)]

48. Rhim, A.D.; Oberstein, P.E.; Thomas, D.H.; Mirek, E.T.; Palermo, C.F.; Sastra, S.A.; Dekleva, E.N.; Saunders, T.; Becerra, C.P.; Tattersall, I.W.; et al. Stromal Elements Act to Restrain, Rather Than Support, Pancreatic Ductal Adenocarcinoma. *Cancer Cell* **2014**, *25*, 735–747. [[CrossRef](#)]
49. Özdemir, B.C.; Pentcheva-Hoang, T.; Carstens, J.L.; Zheng, X.; Wu, C.-C.; Simpson, T.R.; Laklai, H.; Sugimoto, H.; Kahlert, C.; Novitskiy, S.V.; et al. Depletion of Carcinoma-Associated Fibroblasts and Fibrosis Induces Immunosuppression and Accelerates Pancreas Cancer with Reduced Survival. *Cancer Cell* **2014**, *25*, 719–734. [[CrossRef](#)] [[PubMed](#)]
50. Norberg, K.J.; Liu, X.; Moro, C.F.; Strell, C.; Nania, S.; Blümel, M.; Balboni, A.; Bozóky, B.; Heuchel, R.L.; Löhr, J.M. A novel pancreatic tumour and stellate cell 3D co-culture spheroid model. *BMC Cancer* **2020**, *20*, 1–13. [[CrossRef](#)] [[PubMed](#)]
51. Kim, S.-K.; Jang, S.D.; Kim, H.; Chung, S.; Park, J.K.; Kuh, H.-J. Phenotypic Heterogeneity and Plasticity of Cancer Cell Migration in a Pancreatic Tumor Three-Dimensional Culture Model. *Cancers* **2020**, *12*, 1305. [[CrossRef](#)]
52. Broekgaarden, M.; Anbil, S.; Bulin, A.-L.; Obaid, G.; Mai, Z.; Baglo, Y.; Rizvi, I.; Hasan, T. Modulation of redox metabolism negates cancer-associated fibroblasts-induced treatment resistance in a heterotypic 3D culture platform of pancreatic cancer. *Biomaterials* **2019**, *222*, 119421. [[CrossRef](#)]
53. Karimnia, V.; Rizvi, I.; Slack, F.J.; Celli, J.P. Photodestruction of Stromal Fibroblasts Enhances Tumor Response to PDT in 3D Pancreatic Cancer Coculture Models. *Photochem. Photobiol.* **2020**, 13339. [[CrossRef](#)] [[PubMed](#)]
54. Gioeli, D.; Snow, C.J.; Simmers, M.B.; Hoang, S.A.; Figler, R.A.; Allende, J.A.; Roller, D.G.; Parsons, J.T.; Wulfkühle, J.D.; Petricoin, E.F.; et al. Development of a multicellular pancreatic tumor microenvironment system using patient-derived tumor cells. *Lab Chip* **2019**, *19*, 1193–1204. [[CrossRef](#)]
55. Di Maggio, F.; Arumugam, P.; Delvecchio, F.R.; Batista, S.; Lechertier, T.; Hodivala-Dilke, K.; Kocher, H.M. Pancreatic stellate cells regulate blood vessel density in the stroma of pancreatic ductal adenocarcinoma. *Pancreatol* **2016**, *16*, 995–1004. [[CrossRef](#)]
56. Gupta, P.; Pérez-Mancera, P.A.; Kocher, H.; Nisbet, A.; Schettino, G.; Velliou, E.G. A Novel Scaffold-Based Hybrid Multicellular Model for Pancreatic Ductal Adenocarcinoma—Toward a Better Mimicry of the in vivo Tumor Microenvironment. *Front. Bioeng. Biotechnol.* **2020**, *8*, 290. [[CrossRef](#)] [[PubMed](#)]
57. Lai, B.F.L.; Lu, R.X.Z.; Hu, Y.; Huyer, L.D.; Dou, W.; Wang, E.Y.; Radulovich, N.; Tsao, M.S.; Sun, Y.; Radisic, M. Recapitulating Pancreatic Tumor Microenvironment through Synergistic Use of Patient Organoids and Organ-on-a-Chip Vasculature. *Adv. Funct. Mater.* **2020**. [[CrossRef](#)]
58. Tsai, S.; McOlash, L.; Palen, K.; Johnson, B.; Duris, C.; Yang, Q.; Dwinell, M.B.; Hunt, B.; Evans, D.B.; Gershan, J.; et al. Development of primary human pancreatic cancer organoids, matched stromal and immune cells and 3D tumor microenvironment models. *BMC Cancer* **2018**, *18*, 1–13. [[CrossRef](#)] [[PubMed](#)]
59. Kuen, J.; Darowski, D.; Kluge, T.; Majety, M. Pancreatic cancer cell/fibroblast co-culture induces M2 like macrophages that influence therapeutic response in a 3D model. *PLoS ONE* **2017**, *12*, e0182039. [[CrossRef](#)]
60. Tang, J.; Cui, J.; Chen, R.; Guo, K.; Kang, X.; Li, Y.; Gao, D.; Sun, L.; Xu, C.; Chen, J.; et al. A three-dimensional cell biology model of human hepatocellular carcinoma in vitro. *Tumor Biol.* **2010**, *32*, 469–479. [[CrossRef](#)]
61. Carpenedo, R.L.; Sargent, C.Y.; McDevitt, T.C. Rotary Suspension Culture Enhances the Efficiency, Yield, and Homogeneity of Embryoid Body Differentiation. *Stem Cells* **2007**, *25*, 2224–2234. [[CrossRef](#)]
62. Brancato, V.; Comunanza, V.; Imparato, G.; Corà, D.; Urciuolo, F.; Noghero, A.; Bussolino, F.; Netti, P.A. Bioengineered tumoral microtissues recapitulate desmoplastic reaction of pancreatic cancer. *Acta Biomater.* **2017**, *49*, 152–166. [[CrossRef](#)]
63. Kirstein, M.N.; Brundage, R.C.; Moore, M.M.; Williams, B.W.; Hillman, L.A.; Dagit, J.W.; Fisher, J.E.; Marker, P.H.; Kratzke, R.A.; Yee, D. Pharmacodynamic characterization of gemcitabine cytotoxicity in an in vitro cell culture bioreactor system. *Cancer Chemother. Pharmacol.* **2007**, *61*, 291–299. [[CrossRef](#)]
64. Candini, O.; Grisendi, G.; Foppiani, E.M.; Brogli, M.; Aramini, B.; Masciale, V.; Spano, C.; Petrachi, T.; Veronesi, E.; Conte, P.; et al. A Novel 3D In Vitro Platform for Pre-Clinical Investigations in Drug Testing, Gene Therapy, and Immuno-oncology. *Sci. Rep.* **2019**, *9*, 1–12. [[CrossRef](#)]
65. Bjånes, T.; Kotopoulis, S.; Murvold, E.T.; Kamčeva, T.; Gjertsen, B.T.; Gilja, O.H.; Schjøtt, J.; Riedel, B.; McCormack, E. Ultrasound- and Microbubble-Assisted Gemcitabine Delivery to Pancreatic Cancer Cells. *Pharmaceutics* **2020**, *12*, 141. [[CrossRef](#)]
66. Mandrycky, C.; Wang, Z.; Kim, K.; Kim, D.-H. 3D bioprinting for engineering complex tissues. *Biotechnol. Adv.* **2016**, *34*, 422–434. [[CrossRef](#)] [[PubMed](#)]
67. Asghar, W.; El Assal, R.; Shafiee, H.; Pitteri, S.; Paulmurugan, R.; Demirci, U. Engineering cancer microenvironments for in vitro 3-D tumor models. *Mater. Today* **2015**, *18*, 539–553. [[CrossRef](#)] [[PubMed](#)]
68. Langer, E.M.; Allen-Petersen, B.L.; King, S.M.; Kendsersky, N.D.; Turnidge, M.A.; Kuziel, G.M.; Riggers, R.; Samatham, R.; Amery, T.S.; Jacques, S.L.; et al. Modeling Tumor Phenotypes In Vitro with Three-Dimensional Bioprinting. *Cell Rep.* **2019**, *26*, 608–623. [[CrossRef](#)] [[PubMed](#)]
69. Hakobyan, D.; Médina, C.; Dusserre, N.; Stachowicz, M.-L.; Handschin, C.; Fricain, J.-C.; Guillermet-Guibert, J.; Oliveira, H. Laser-assisted 3D bioprinting of exocrine pancreas spheroid models for cancer initiation study. *Biofabrication* **2020**, *12*, 035001. [[CrossRef](#)]
70. Conchello, J.-A.; Lichtman, J.W. Optical sectioning microscopy. *Nat. Methods* **2005**, *2*, 920–931. [[CrossRef](#)] [[PubMed](#)]
71. Mertz, J. Optical sectioning microscopy with planar or structured illumination. *Nat. Methods* **2011**, *8*, 811–819. [[CrossRef](#)]
72. Reynaud, E.G.; Kržič, U.; Greger, K.; Stelzer, E.H.K. Light sheet-based fluorescence microscopy: More dimensions, more photons, and less photodamage. *HFSP J.* **2008**, *2*, 266–275. [[CrossRef](#)]

73. Pampaloni, F.; Reynaud, E.G.; Stelzer, E.H.K. The third dimension bridges the gap between cell culture and live tissue. *Nat. Rev. Mol. Cell Biol.* **2007**, *8*, 839–845. [[CrossRef](#)]
74. Beer, M.; Kuppala, N.; Stefanini, M.; Becker, H.; Schulz, I.; Manoli, S.; Schuette, J.; Schmees, C.; Casazza, A.; Stelzle, M.; et al. A novel microfluidic 3D platform for culturing pancreatic ductal adenocarcinoma cells: Comparison with in vitro cultures and in vivo xenografts. *Sci. Rep.* **2017**, *7*, 1–12. [[CrossRef](#)]
75. Bradney, M.J.; Venis, S.M.; Yang, Y.; Konieczny, S.F.; Han, B. A Biomimetic Tumor Model of Heterogeneous Invasion in Pancreatic Ductal Adenocarcinoma. *Small* **2020**, *16*, e1905500. [[CrossRef](#)] [[PubMed](#)]
76. Bi, Y.; Shirure, V.S.; Liu, R.; Cunningham, C.; Ding, L.; Meacham, J.M.; Goedegebuure, S.P.; George, S.C.; Fields, R.C. Tumor-on-a-chip platform to interrogate the role of macrophages in tumor progression. *Integr. Biol.* **2020**, *12*. [[CrossRef](#)] [[PubMed](#)]
77. Moon, H.-R.; Ozcelikkale, A.; Yang, Y.; Elzey, B.D.; Konieczny, S.F.; Han, B. An engineered pancreatic cancer model with intra-tumoral heterogeneity of driver mutations. *Lab Chip* **2020**, *20*, 3720–3732. [[CrossRef](#)]
78. Kramer, B.; De Haan, L.; Vermeer, M.; Olivier, T.; Hankemeier, T.; Vulto, P.; Joore, J.; Lanz, H.L. Interstitial Flow Recapitulates Gemcitabine Chemoresistance in A 3D Microfluidic Pancreatic Ductal Adenocarcinoma Model by Induction of Multidrug Resistance Proteins. *Int. J. Mol. Sci.* **2019**, *20*, 4647. [[CrossRef](#)]
79. Nguyen, D.-H.T.; Lee, E.; Alimperti, S.; Norgard, R.J.; Wong, A.; Lee, J.J.-K.; Eyckmans, J.; Stanger, B.Z.; Chen, C.S. A biomimetic pancreatic cancer on-chip reveals endothelial ablation via ALK7 signaling. *Sci. Adv.* **2019**, *5*, eaav6789. [[CrossRef](#)]
80. Siret, C.; Collignon, A.; Silvy, F.; Robert, S.; Cheyrol, T.; André, P.; Rigot, V.; Iovanna, J.; Van De Pavert, S.; Lombardo, D.; et al. Deciphering the Crosstalk Between Myeloid-Derived Suppressor Cells and Regulatory T Cells in Pancreatic Ductal Adenocarcinoma. *Front. Immunol.* **2020**, *10*, 3070. [[CrossRef](#)]
81. Gresham, G.K.; Wells, G.; Gill, S.; Cameron, C.; Jonker, D.J. Chemotherapy regimens for advanced pancreatic cancer: A systematic review and network meta-analysis. *BMC Cancer* **2014**, *14*, 471. [[CrossRef](#)]
82. Conroy, T.; Desseigne, F.; Ychou, M.; Bouché, O.; Guimbaud, R.; Bécouarn, Y.; Adenis, A.; Raoul, J.-L.; Gourgou-Bourgade, S.; de la Fouchardière, C.; et al. FOLFIRINOX versus Gemcitabine for Metastatic Pancreatic Cancer. *N. Engl. J. Med.* **2011**, *364*, 1817–1825. [[CrossRef](#)] [[PubMed](#)]
83. Murakami, T.; Hiroshima, Y.; Matsuyama, R.; Homma, Y.; Hoffman, R.M.; Endo, I. Role of the tumor microenvironment in pancreatic cancer. *Ann. Gastroenterol. Surg.* **2019**, *3*, 130–137. [[CrossRef](#)] [[PubMed](#)]
84. Seton-Rogers, S. Fibroblasts shape PDAC architecture. *Nat. Rev. Cancer* **2019**, *19*, 418. [[CrossRef](#)] [[PubMed](#)]
85. Adisheshaiah, P.P.; Crist, R.M.; Hook, S.S.; McNeil, S.E. Nanomedicine strategies to overcome the pathophysiological barriers of pancreatic cancer. *Nat. Rev. Clin. Oncol.* **2016**, *13*, 750–765. [[CrossRef](#)] [[PubMed](#)]
86. Brachi, G.; Bussolino, F.; Ciardelli, G.; Mattu, C. Nanomedicine for Imaging and Therapy of Pancreatic Adenocarcinoma. *Front. Bioeng. Biotechnol.* **2019**, *7*, 307. [[CrossRef](#)] [[PubMed](#)]
87. Van Der Meel, R.; Sulheim, E.; Shi, Y.; Kiessling, F.; Mulder, W.J.M.; Lammers, T. Smart cancer nanomedicine. *Nat. Nanotechnol.* **2019**, *14*, 1007–1017. [[CrossRef](#)]
88. Jang, H.L.; Sengupta, S. Transcellular transfer of nanomedicine. *Nat. Nanotechnol.* **2019**, *14*, 731–732. [[CrossRef](#)]
89. Al-Batran, S.-E.; Geissler, M.; Seufferlein, T.; Oettle, H. Nab-Paclitaxel for Metastatic Pancreatic Cancer: Clinical Outcomes and Potential Mechanisms of Action. *Oncol. Res. Treat.* **2014**, *37*, 128–134. [[CrossRef](#)]
90. Wang-Gillam, A.; Hubner, R.A.; Siveke, J.T.; Von Hoff, D.D.; Belanger, B.; de Jong, F.A.; Mirakhur, B.; Chen, L.-T. NAPOLI-1 phase 3 study of liposomal irinotecan in metastatic pancreatic cancer: Final overall survival analysis and characteristics of long-term survivors. *Eur. J. Cancer* **2019**, *108*, 78–87. [[CrossRef](#)]
91. Zhang, B.; Jiang, T.; Shen, S.; She, X.; Tuo, Y.; Hu, Y.; Pang, Z.; Jiang, X. Cyclopamine disrupts tumor extracellular matrix and improves the distribution and efficacy of nanotherapeutics in pancreatic cancer. *Biomaterials* **2016**, *103*, 12–21. [[CrossRef](#)]
92. Ray, P.; Confeld, M.; Borowicz, P.; Wang, T.; Mallik, S.; Quadir, M. PEG-b-poly (carbonate)-derived nanocarrier platform with pH-responsive properties for pancreatic cancer combination therapy. *Colloids Surf. B Biointerfaces* **2019**, *174*, 126–135. [[CrossRef](#)]
93. Oluwasanmi, A.; Al-Shakarchi, W.; Manzur, A.; Aldebasi, M.H.; Elsin, R.S.; Albusair, M.K.; Haxton, K.J.; Curtis, A.D.; Hoskins, C. Diels Alder-mediated release of gemcitabine from hybrid nanoparticles for enhanced pancreatic cancer therapy. *J. Control. Release* **2017**, *266*, 355–364. [[CrossRef](#)] [[PubMed](#)]
94. Wason, M.S.; Colon, J.; Das, S.; Seal, S.; Turkson, J.; Zhao, J.; Baker, C.H. Sensitization of pancreatic cancer cells to radiation by cerium oxide nanoparticle-induced ROS production. *Nanomedicine Nanotechnol. Biol. Med.* **2013**, *9*, 558–569. [[CrossRef](#)]
95. Tummers, W.S.; Bs, S.E.M.; Teraphongphom, N.T.; Gomez, A.; Steinberg, I.; Huland, D.M.; Hong, S.; Kothapalli, S.-R.; Hasan, A.; Ertsey, R.; et al. Intraoperative Pancreatic Cancer Detection using Tumor-Specific Multimodality Molecular Imaging. *Ann. Surg. Oncol.* **2018**, *25*, 1880–1888. [[CrossRef](#)] [[PubMed](#)]
96. Hoogstins, C.E.S.; Boogerd, L.S.F.; Bsc, B.G.S.M.; Mieog, J.S.D.; Swijnenburg, R.J.; Van De Velde, C.J.H.; Sarasqueta, A.F.; Bonsel, B.A.; Framery, B.; Pèlerin, A.; et al. Image-Guided Surgery in Patients with Pancreatic Cancer: First Results of a Clinical Trial Using SGM-101, a Novel Carcinoembryonic Antigen-Targeting, Near-Infrared Fluorescent Agent. *Ann. Surg. Oncol.* **2018**, *25*, 3350–3357. [[CrossRef](#)]
97. Perlman, O.; Weitz, I.S.; Azhari, H. Copper oxide nanoparticles as contrast agents for MRI and ultrasound dual-modality imaging. *Phys. Med. Biol.* **2015**, *60*, 5767–5783. [[CrossRef](#)] [[PubMed](#)]

98. Handgraaf, H.J.M.; Boonstra, M.C.; Van Erkel, A.R.; Bonsing, B.A.; Putter, H.; Van De Velde, C.J.H.; Vahrmeijer, A.L.; Mieog, J.S.D. Current and Future Intraoperative Imaging Strategies to Increase Radical Resection Rates in Pancreatic Cancer Surgery. *BioMed Res. Int.* **2014**, *2014*, 1–8. [[CrossRef](#)]
99. Wang, Q.; Zhu, X.; Wu, Z.; Sun, T.; Huang, W.; Wang, Z.; Ding, X.; Jiang, C.; Li, F. Theranostic nanoparticles enabling the release of phosphorylated gemcitabine for advanced pancreatic cancer therapy. *J. Mater. Chem. B* **2020**, *8*, 2410–2417. [[CrossRef](#)]
100. Rosenberger, I.; Strauss, A.; Dobiasch, S.; Weiß, C.; Szanyi, S.; Gil-Iceta, L.; Alonso, E.; Esparza, M.G.; Gómez-Vallejo, V.; Szczupak, B.; et al. Targeted diagnostic magnetic nanoparticles for medical imaging of pancreatic cancer. *J. Control. Release* **2015**, *214*, 76–84. [[CrossRef](#)]
101. Hilmi, M.; Bartholin, L.; Neuzillet, C. Immune therapies in pancreatic ductal adenocarcinoma: Where are we now? *World J. Gastroenterol.* **2018**, *24*, 2137–2151. [[CrossRef](#)]
102. Nakamura, T.; Harashima, H. Integration of nano drug-delivery system with cancer immunotherapy. *Ther. Deliv.* **2017**, *8*, 987–1000. [[CrossRef](#)]
103. Manolova, V.; Flace, A.; Bauer, M.; Schwarz, K.; Saudan, P.; Bachmann, M.F. Nanoparticles target distinct dendritic cell populations according to their size. *Eur. J. Immunol.* **2008**, *38*, 1404–1413. [[CrossRef](#)]
104. Dermani, F.K.; Samadi, P.; Rahmani, G.; Kohlan, A.K.; Najafi, R. PD-1/PD-L1 immune checkpoint: Potential target for cancer therapy. *J. Cell. Physiol.* **2019**, *234*, 1313–1325. [[CrossRef](#)]
105. Miao, L.; Li, J.; Liu, Q.; Feng, R.; Das, M.; Lin, C.M.; Goodwin, T.J.; Dorosheva, O.; Liu, R.; Huang, L. Transient and Local Expression of Chemokine and Immune Checkpoint Traps To Treat Pancreatic Cancer. *ACS Nano* **2017**, *11*, 8690–8706. [[CrossRef](#)] [[PubMed](#)]
106. Labadie, B.W.; Bao, R.; Luke, J.J. Reimagining IDO Pathway Inhibition in Cancer Immunotherapy via Downstream Focus on the Tryptophan–Kynurenine–Aryl Hydrocarbon Axis. *Clin. Cancer Res.* **2019**, *25*, 1462–1471. [[CrossRef](#)] [[PubMed](#)]
107. Lu, J.; Liu, X.; Liao, Y.-P.; Salazar, F.; Sun, B.; Jiang, W.; Chang, C.H.; Jiang, J.; Wang, X.; Wu, A.M.; et al. Nano-enabled pancreas cancer immunotherapy using immunogenic cell death and reversing immunosuppression. *Nat. Commun.* **2017**, *8*, 1–14. [[CrossRef](#)]
108. Zhao, X.; Li, F.; Li, Y.; Wang, H.; Ren, H.; Chen, J.; Nie, G.; Hao, J. Co-delivery of HIF1 α siRNA and gemcitabine via biocompatible lipid-polymer hybrid nanoparticles for effective treatment of pancreatic cancer. *Biomaterials* **2015**, *46*, 13–25. [[CrossRef](#)] [[PubMed](#)]
109. Ellah, N.H.A.; Abouelmagd, S.A. Surface functionalization of polymeric nanoparticles for tumor drug delivery: Approaches and challenges. *Expert Opin. Drug Deliv.* **2017**, *14*, 201–214. [[CrossRef](#)]
110. Wu, C.Y.; Pu, Y.; Liu, G.; Shao, Y.; Ma, Q.S.; Zhang, X.M. MR imaging of human pancreatic cancer xenograft labeled with superparamagnetic iron oxide in nude mice. *Contrast Media Mol. Imaging* **2012**, *7*, 51–58. [[CrossRef](#)]
111. Darrigues, E.; Dantuluri, V.; Nima, Z.A.; Vang-Dings, K.B.; Griffin, R.J.; Biris, A.R.; Ghosh, A. Raman spectroscopy using plasmonic and carbon-based nanoparticles for cancer detection, diagnosis, and treatment guidance. Part 2: Treatment. *Drug Metab. Rev.* **2017**, *49*, 253–283. [[CrossRef](#)]
112. Managò, S.; Migliaccio, N.; Terracciano, M.; Napolitano, M.; Martucci, N.M.; De Stefano, L.; Rendina, I.; De Luca, A.C.; Lamberti, A.; Rea, I. Internalization kinetics and cytoplasmic localization of functionalized diatomite nanoparticles in cancer cells by Raman imaging. *J. Biophotonics* **2018**, *11*, e201700207. [[CrossRef](#)] [[PubMed](#)]
113. Durr, N.J.; Larson, T.; Smith, D.K.; Korgel, B.A.; Sokolov, K.; Ben-Yakar, A. Two-Photon Luminescence Imaging of Cancer Cells Using Molecularly Targeted Gold Nanorods. *Nano Lett.* **2007**, *7*, 5. [[CrossRef](#)]
114. Phan, T.T.V.; Bui, N.Q.; Cho, S.-W.; Bharathiraja, S.; Manivasagan, P.; Moorthy, M.S.; Mondal, S.; Kim, C.-S.; Oh, J. Photoacoustic Imaging-Guided Photothermal Therapy with Tumor-Targeting HA-FeOOH@PPy Nanorods. *Sci. Rep.* **2018**, *8*, 1–13. [[CrossRef](#)]
115. Lazzari, G.; Vinciguerra, D.; Balasso, A.; Nicolas, V.; Goudin, N.; Garfa-Traore, M.; Féher, A.; Dinnyés, A.; Nicolas, J.; Couvreur, P.; et al. Light sheet fluorescence microscopy versus confocal microscopy: In quest of a suitable tool to assess drug and nanomedicine penetration into multicellular tumor spheroids. *Eur. J. Pharm. Biopharm.* **2019**, *142*, 195–203. [[CrossRef](#)] [[PubMed](#)]
116. Darrigues, E.; Nima, Z.A.; Nedosekin, D.A.; Watanabe, F.; Alghazali, K.M.; Zharov, V.P.; Biris, A.S. Tracking Gold Nanorods' Interaction with Large 3D Pancreatic-Stromal Tumor Spheroids by Multimodal Imaging: Fluorescence, Photoacoustic, and Photothermal Microscopies. *Sci. Rep.* **2020**, *10*, 1–14. [[CrossRef](#)] [[PubMed](#)]